

Research Article

# Effect of Sol-gel Coating on Microscopic, Thermal and Water Absorption Behavior of Aramid/Nylon 6/6/Nanodiamond-based Fibers

Ayesha Kausar<sup>1,\*</sup>

<sup>1</sup>Nanosciences and Catalysis Division, National Centre For Physics, Quaid-i-Azam University Campus, Islamabad, Pakistan

## Abstract

In this article, an aramid of 4,4'-(1,3-phenylenedioxy)dianiline and terephthaloyl chloride was prepared. Afterwards, Nylon 6/6 and aramid were used to prepare sol-gel coated and non-coated blend fibers reinforced with nanodiamond (ND). In this way, four types of fibers were fabricated i.e. aramid/Nylon 6/6 fibers (Ar/N66) and aramid/Nylon 6/6/nanodiamond fibers (Ar/N66//ND) and sol-gel coated s-Ar/N66 and s-Ar/N66//ND fibers. The fibers were fabricated *via* Brabender single screw extruder at 200 °C. The Ar/N66 and Ar/N66//ND fibers were coated by means of simple dip-coating technique. Fourier transform infrared spectroscopy was used for structural characterization. Scanning electron microscopic images of non-coated and sol-gel coated fibers were scanned for morphological comparison. Glass transition temperature of the sol gel s-Ar/N66 fibers increased up to 232 °C, while that of s-Ar/N66//ND was enhanced to 240 °C relative to neat fibers. Moreover, the sol-gel coated s-Ar/N66//ND (8.08%) fibers had higher water absorbing tendency than non-coated Ar/N66//ND (7.66 %).

**Keywords:** Aramid; Nylon 6/6; sol-gel; fiber; nanodiamond; water uptake

**Academic Editor:** Taihong Shi, PhD, PhD, Sun Yat-sen University, China

**Received:** August 14, 2015; **Accepted:** September 29, 2015; **Published:** October 8, 2015

Competing Interests: The authors have declared that no competing interests exist.

**Copyright:** 2015 Kausar A. This is an open-access article distributed under the terms of the Creative Commons Attribution License, which permits unrestricted use, distribution, and reproduction in any medium, provided the original author and source are credited.

**\*Correspondence to:** Ayesha Kausar, Nanosciences and Catalysis Division, National Centre For Physics, Quaid-i-Azam University Campus, Islamabad, Pakistan; **Email:** [asheesgreat@yahoo.com](mailto:asheesgreat@yahoo.com)

## 1. Introduction

Aramid fibers are a category of synthetic and strongly heat-resilient fibers [1]. In such fibers, the molecular chains are arranged alongside the fiber axis; hence the chemical bond strength can be maneuvered. Initially with a *meta*-aramid fiber, aromatic polyamides were instigated in commercial requisitions designed by DuPont as Nomex [2]. The fiber, which works like ordinary textile wear fibers, was described by its excellent heat resistance, as it neither melts down nor erupts under ordinary oxygen levels. It is widely used in the synthesis of apparel, protective air filtration, electrical, and thermal insulation as well as a substitute to asbestos. Aramid fibers are being used gradually in a broad spectrum of applications owing to their high modulus, high specific strength, low density, and high thermal resilience of aramid [3]. By reacting amine group and carboxylic acid halide group, aramids (aromatic polyamides) are usually manufactured [4]. After the production of polymer, the aramid fiber is synthesized by blending the liquefied polymer to solid fiber, by liquid chemical blend. For spinning purpose, polymer solvent is normally 100% anhydrous sulfuric acid. Additional variations are related to the range of aramid fibers besides *meta*- and *para*-aramid [5]. Such moderately simple procedure consumes only single amide solvent, and hence spinning can be performed directly after the formation of polymer. The long-standing service in insensitive environment is preferred when employed in space and aviation engineering. The properties of aramid fiber mark it suitable for numerous industries. It can be present in optical fiber, cables, linear tension members, ballistics, conveyer and transmission belts, tires, as well as cut and heat protection [6]. Due to its less stiffness, density and high resilience to destruction, it is widely utilized in the transportation and marine industries for manufacture of stronger, stiffer, lighter, and many more long-lasting parts [7]. Oxide or oxide-based coatings have been layered on several substrate resources through sol-gel methods [8]. There are various potential gains of sol-gel procedure for aramid fibers preparation with photo-shielded coating films such as less expense in both the precursors and the coating equipment, low pressure and low temperature processing circumstances, fast output and no destruction to the substrate resources. Additionally during the course of processing the large area films can be simply manufactured, because the sol-gel route is a liquid-phase procedure. For modification of these 3D structures, the use of sol-gel technique encounters two imperative conditions (*i*) complete surface coating of the substrate is confirmed by the process proceeding in liquid environment and ranges all the sections of the 3D substrate (*ii*) reasonably low temperature (room temperature) and pressure (atmospheric pressure) in all the stages leading to reduction in thermal degradation of the 3D structure [9, 10]. Researchers have also transformed the physical and thermal properties of polymer fibers by composite system manufacture [11-13]. Nanodiamond (ND) produced by detonation production are based on homogeneous and small particles of ~5 nm in diameter and implies an accessible and huge surface area. Bulky diamond has unique properties comprising superior stiffness, thermal conductivity, high refraction index, Young's modulus, hardness, and a high resistivity [14]. There are several research efforts addressing the thermoplastics strengthening with ND. Even without surface modification and at low concentrations, ND has been accounted to strengthen several thermoplastics [15, 16]. In this effort, Nylon 6/6 and aramid of 4,4'-(1,3-phenylenedioxy)dianiline and terephthaloyl chloride were used to produce composite fibers of aramid/Nylon 6/6 fibers (Ar/N66) and aramid/Nylon 6/6/nanodiamond fibers (Ar/N66//ND). Later the fibers were coated using simple sol-gel coating technique. The structure, morphological, thermal and water absorption characteristics of novel fibers have been investigated.

## 2. Experimental

### 2.1. Materials

Nylon 6 (pellets), 4,4'-(1,3-phenylenedioxy)dianiline (98%), terephthaloyl chloride ( $\geq 99\%$ , flakes), diamond nanopowder ( $< 10$  nm particle size), tetraethyl orthosilicate (TEOS, 99.99 %), titanium(IV) isopropoxide (TIP,  $\geq 97$  %) and N,N-dimethylformamide (99 %) were supplied by Aldrich.

### 2.2. Characterization techniques

IR spectra were taken at room temperature with a resolution of  $4\text{ cm}^{-1}$  using Excalibur Series FTIR Spectrometer, Model No. FTSW 300 MX manufactured by BIO-RAD. The scanning electron microscopic (SEM) images were obtained by Scanning Electron Microscope S-4700 (Japan Hitachi Co. Ltd.). Differential scanning calorimetry (DSC) was performed by a METTLER TOLEDO DSC 822 differential scanning calorimeter taking 5 mg of the samples encapsulated in aluminum pans and heated at a rate of  $10\text{ }^{\circ}\text{C}/\text{min}$  under nitrogen atmosphere. Water absorption tendency of the fibers was evaluated by immersing equal weights of the sample films in water for 100 h at ambient temperature. The water uptake was calculated using Eq 1.

$$\% \text{ Water uptake} = \frac{w_2 - w_1}{w_1} \quad (1)$$

Where,

$w_1$ - Initial membrane weight (g)

$w_2$ - Final membrane weight (g)

### 2.3. Preparation of TIP coating

10 mL of TIP was added to 10 mL of absolute ethanol with continuous stirring of 1h. Afterward, 1 mL of TEOS was added to this mixture and stirred for additional 1h. The mixture was then diluted to 50 mL of absolute ethanol.

### 2.4. Preparation of aramid

Equimolar amount of 4,4'-(1,3-phenylenedioxy)dianiline and terephthaloyl chloride were refluxed in 50 mL of DMF for 6 h ( $120\text{ }^{\circ}\text{C}$ ). The mixture was poured into 200 mL of distilled water. The precipitates were filtered and washed with distilled water. FTIR ( $\text{cm}^{-1}$ ): 3230 (N–H stretching vibration), 3009 (Ar C–H stretching vibration), 1692 (C=O amide carbonyl), 1595 (N–H bending vibration).

### 2.5. Preparation of aramid/Nylon 6/6 blend fibers (Ar/N66)

The nylon 6/6 and aramid were dried at  $70\text{ }^{\circ}\text{C}$  for 8 h to remove the moisture content. Then the preferred amount of nylon 6/6 and aramid were placed in Brabender single screw extruder (Intelli-torque) and fibers

were fabricated using a single hole fiber die (diameter = 0.012 inches L/D ratio = 3). The temperature was kept at 200 °C with a screw speed of 3 rpm. The extruded fibers were stretched with Instron fiber clamps at room temperature [17]. FTIR ( $\text{cm}^{-1}$ ): 3219 (N–H stretching vibration), 3001 (Ar C–H stretching vibration), 2982 (aliphatic C–H stretching vibration), 1686 (C=O amide carbonyl), 1590 (N–H bending vibration).

## 2.6. Preparation of aramid/Nylon 6/6/nanodiamond fibers (Ar/N66//ND)

The nylon 6/6, aramid and nanodiamond fibers were prepared using similar procedure mentioned in Section 2.4. The difference was that the desired amount of nanodiamond was also added along with the polyamides.

## 2.7. Sol-gel coating of s-Ar/N66 and s-Ar/N66//ND fibers

The prepared fibers were coated with TIP mixture *via* simple dip-coating technique. The dipping rate was  $50 \text{ mm min}^{-1}$ , while the immersion time was kept 1h for all the fibers. The number of deposited layers was 1, 5, or 10. After deposition, the samples were washed and dried at 80 °C for 24 h (Fig. 1). FTIR ( $\text{cm}^{-1}$ ): 3233 (N–H stretching vibration), 3004 (Ar C–H stretching vibration), 2980 (aliphatic C–H stretching vibration), 1692 (C=O amide carbonyl), 1595 (N–H bending vibration), 1025 (Si–O–Si asymmetric stretching), 920 (Si–OH), 802 (Si–O–Si symmetric stretching), 461 (Si–O–Si bending mode).

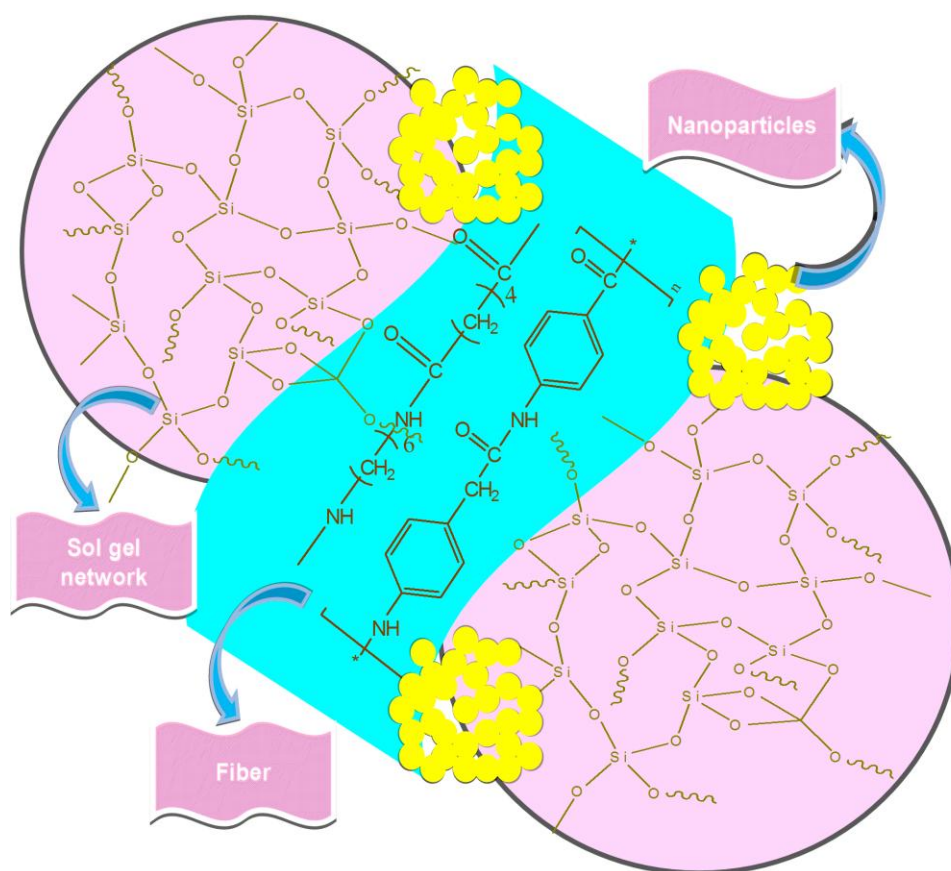


**Fig. 1** A schematic diagram for sol-gel coated Ar/N66//ND fiber.

### 3. Results and Discussion

#### 3.1. Microscopic studies

FESEM images of fractured surfaces of Ar/N66, s-Ar/N66, Ar/N66//ND, and s-Ar/N66//ND fibers are given in Fig. 2. The micrographs illustrated that the neat polyamide blend fibers without any sol-gel coating possess leveled surface without any aggregation or particulate matter (Fig. 2A & C). Micrographs depict uniform alignment of the fabricated fibers. Fig. 2B showed that the sol-gel coated polyamide blend/nanodiamond fibers were uniformly oriented. However, the sol-gel coating over the fiber surface caused a bit increase in the fiber diameter. The s-Ar/N66//ND fibers were also uniformly aligned with somewhat coarse surface (Fig. 2D). In sol-gel coated fibers, the fiber pull out phenomenon was also observed on the fractured surface. The fiber pull out was probably due to the increased rigidity of the fibers. However no the interface de-bonding, cracking, or delamination was experiential in sol-gel coated s-Ar/N66 and s-Ar/N66//ND fibers.

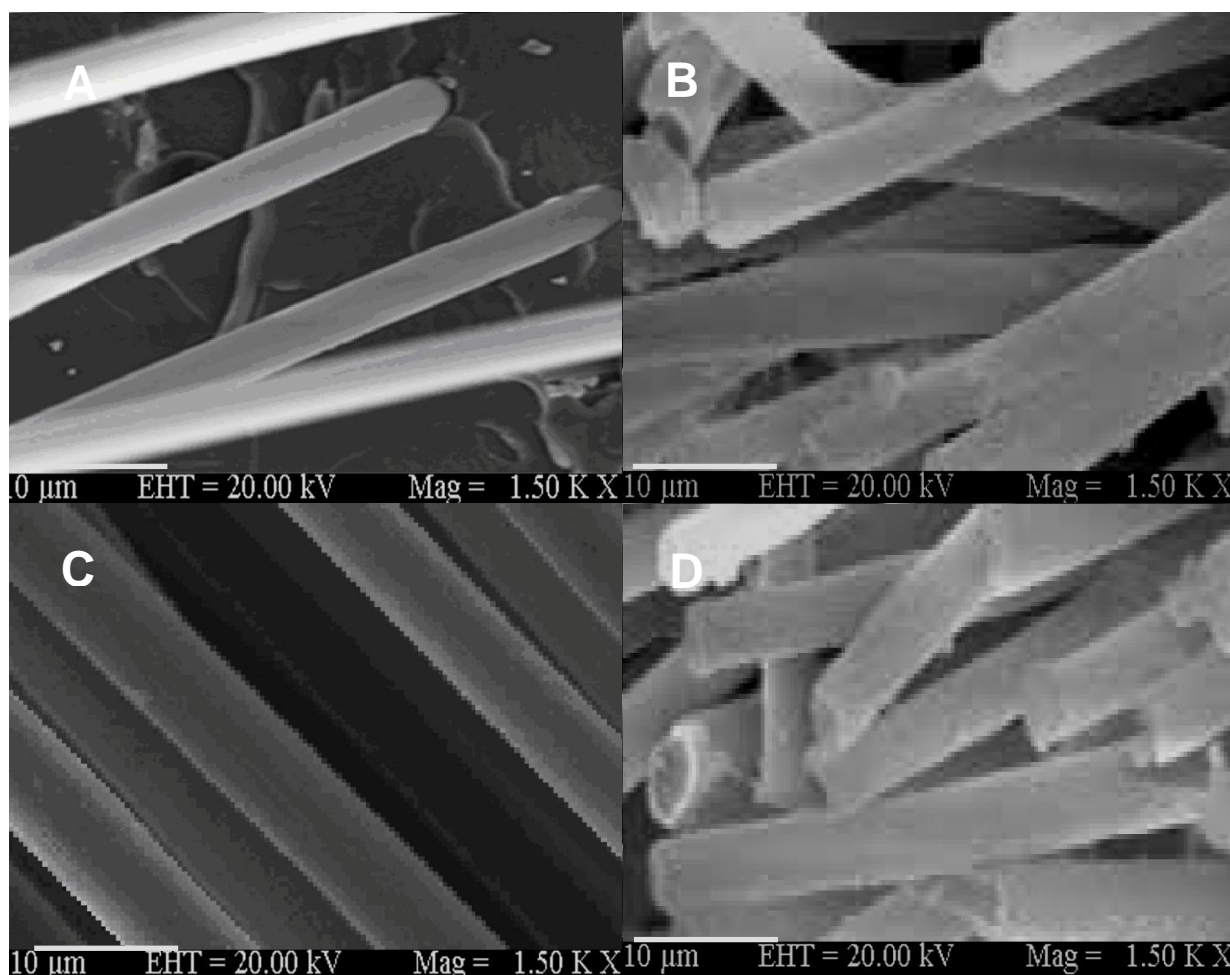


**Fig. 2** FESEM images of (A) Ar/N66; (B) s-Ar/N66; (C) Ar/N66//ND; and (D) s-Ar/N66//ND.

### 3.2. Glass transition of polyamide blend and composite fiber

The fiber melting was studied by DSC. The thermograms of Ar/N66, Ar/N66//ND, s-Ar/N66 and s-Ar/N66//ND fibers were recorded at heating rate of 10 °C/min in N<sub>2</sub>. The DSC traces of the samples are compared in Fig. 3. A summary of the DSC data corresponding to the curves for the heating scan are tabulated in Table 1. The data indicated that the peaks of the sol-gel coated fibers were shifted towards right. The glass transition temperature ( $T_g$ ) was also enhanced from 226 °C in Ar/N66 to 232 °C in s-Ar/N66. For s-Ar/N66//ND, the  $T_g$  was 240 °C relative to Ar/N66//ND (235 °C). The obvious fact was the sol-gel network coating on polyamide fibers that caused an increase in the rigidity/crystallinity of nanocomposite. The silanol groups were mainly accountable for this increased firmness of polyamide blend fibers. The incorporation of nanodiamond particles within the chain interstices also increased the overall rigidity possibly by enhancing the interaction with the polyamide backbone. Comparable results were found in literature for polyamide/silica nanocomposite [18, 19]. In these novel polyamide nanocomposite fibers, the glass transition temperature was increased by sol-gel dip coating technique.

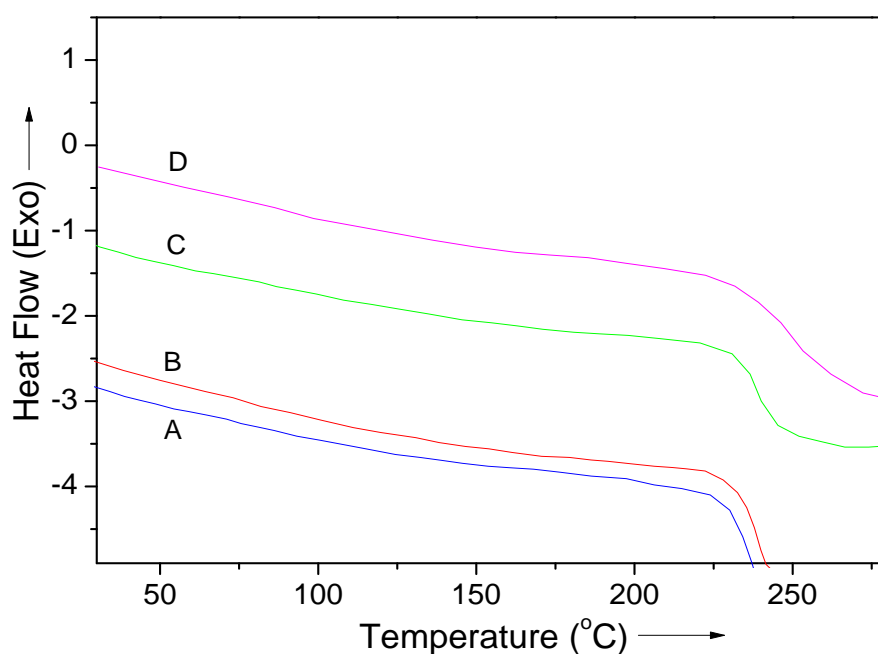


**Fig. 3** DSC thermograms of (A) Ar/N66; (B) s-Ar/N66; (C) Ar/N66//ND; and (D) s-Ar/N66//ND at 10 °C/min in N<sub>2</sub>.

**Table 1** Glass transition temperature and % water uptake of sol-gel coated fibers.

Samples	$T_g$ (°C)	Water uptake (%)
Ar/N66	226	6.21
s-Ar/N66	232	7.18
Ar/N66//ND	235	7.66
s-Ar/N66//ND	240	8.08

### 3.3. Water absorption behavior

The water uptake characteristics of Ar/N66, Ar/N66//ND, and sol-gel coated s-Ar/N66 and s-Ar/N66//ND fibers were studied (Table 1). Fig. 4 shows the comparative water uptake distinctiveness of the polyamide blend-based fibers. It was experiential that the non-coated Ar/N66 and Ar/N66//ND have water uptake of 6.21 and 7.66 % respectively. On the other hand, the constitution of sol-gel coated polyamide blend appears to be hydrophilic and apt to soak up water effortlessly. The s-Ar/N66 and s-Ar/N66//ND fibers therefore have higher % water uptake of 7.18 and 8.08 respectively. Consequently, the sol-gel fibers depicted higher water uptake compared with the other fibers. The tendency can be explained on the basis of sol-gel network formation [20, 21]. Results revealed that the incorporation of nanodiamond in the fibers also render them more hydrophilic as Ar/N66//ND was more water absorbing compared with Ar/N66. It was perceived that the sol-gel network structure led to the formation of porous structure over the fiber surface.

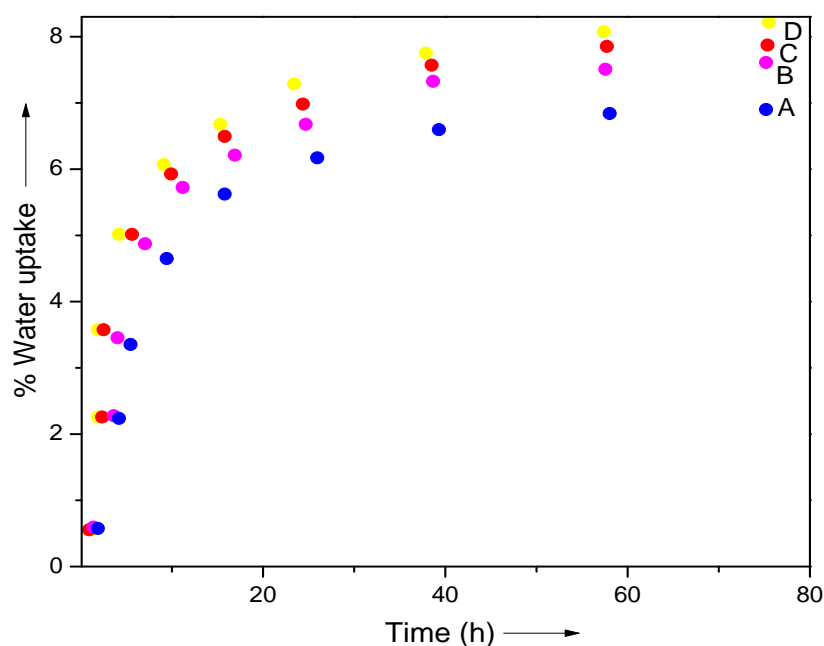


Fig. 4 Water uptake characteristics of (A) Ar/N66; (B) s-Ar/N66; (C) Ar/N66//ND; and (D) s-Ar/N66//ND.

## 4. Conclusion

The polyamide fibers with notable physical properties were employed as talented material for a wide range of technical applications. In this work, silica and nanodiamond were introduced as low-cost inorganic and organic nanofiller for polyamide blend fibers. Brabender single screw extruder technique was used to prepare aramid and nylon 6/6 blend-based fibers. The sol-gel coating was done using dipping process. The sol-gel network on the fiber surface developed better compatibility with aramid and polyamide 6/6 containing nanodiamond in matrix. The sol-gel composite fibers own increased glass transition temperature as characterized by DSC. Morphology study revealed homogeneously aligned fiber formation. The sol-gel

coated fibers also supported greater water absorption compared with the non-coated polyamide blend fibers.

## References

1. Kausar A. Properties of Sol-gel Coated Fibers of Polyamide 6/12/Polyvinylpyrrolidone/Nanodiamond. *Int J Mater Chem*. 2015, 5, 91-95.
2. Demircan O, Kosui T, Ashibe S, Nakai A. Effect of Stitch and Biaxial Yarn Types on Tensile, Bending and Impact Properties of Biaxial Weft Knitted Composites. *Adv Compos Mater*. 2014, 23, 239-260
3. Zhao X, Hirogaki K, Tabata I, Okubayashi S, Horia T. A new method of producing conductive aramid fibers using supercritical carbon dioxide. *Surf Coat Tech*. 2006, 201, 628-636
4. Kausar A. Mechanical thermal and electrical properties of epoxy matrix composites reinforced with polyamide-grafted-MWCNT/poly (azo-pyridine-benzophenone-imide)/polyaniline nanofibers. *Int J Polym Mater*. 2014, 63, 831-839
5. Derombise G, Schoors L V V, Davies P. Degradation of Technora aramid fibres in alkaline and neutral environments. *Polym Degrad Stab*. 2009, 94, 1615-1620
6. Kausar A. Polyamide-Grafted-Multi-walled Carbon Nanotube Electrospun Nanofibers/Epoxy Composites. *Fibers Polym*. 2014, 15, 2564-2571
7. Song YS, Oh H, Jeong TT, Youn JR. A novel manufacturing method for carbon nanotube/aramid fiber filled hybrid multi-component composites. *Adv Compos Mater*. 2008, 17, 333-341
8. Wen J, Wilkes GL. Synthesis and characterization of abrasion resistant coating materials prepared by the sol-gel approach: I. Coatings based on functionalized aliphatic diols and diethylenetriamine. *J Inorg Organometal Polym*. 1995, 5, 343-375
9. Kausar A. Composites of Sulfonated Polystyrene-*block*-Poly(ethylene-*ran*-butylene)-*block*-Polystyrene and Graphite-Polyoxometalate: Preparation, Thermal and Electrical Conductivity. *Int J Mater Chem* 2015, 5, 85-90.
10. Bandeira LC, Ciuffi KJ, Calefi, PS, Nassar EJ, Salvado IMM, Fernandes MHFV. Low temperature synthesis of bioactive materials. *Ceramica*. 2011, 57, 166-167
11. Yang XF, Li QL, Chen ZP, Zhang L, Zhou Y. Mechanism studies of thermolysis process in copolyamide 66 containing triaryl phosphine oxide. *J Therm Anal Calorim*. 2013, 112, 567-571
12. Karsli NG, Yilmaz T, Aytac A, Ozkoc G. Investigation of erosive wear behavior and physical properties of SGF and/or calcite reinforced ABS/PA6 composites. *Composite Part B*. 2013, 44, 385-393
13. Czegeny Z, Jakab E, Blazso M, Bhaskar T, Sakata Y. Thermal decomposition of polymer mixtures of PVC, PET and ABS containing brominated flame retardant: formation of chlorinated and brominated organic compounds. *J Anal Appl Pyrol*. 2012, 96, 69-77
14. Kausar A. Preparation and Characteristics of Mercaptobenzene Functionalized Graphite and Epoxy-based Hybrid Membranes. *Am J Mater Sci* 2015, 5, 17-21
15. Kausar A. Nanodiamond/MWCNT-based Polymeric Nanofiber Reinforced Poly(Bisphenol A-co-epichlorohydrin). *Malaysian Polym J* 2015, 10, 23-32.
16. Kausar A. Polyaniline Composites with Nanodiamond, Carbon nanotube and Silver Nanoparticle: Preparation and Properties. *Am J Polym Sci Engineer* 2015, 3, 149-160.

17. Kausar A, Hussain ST. Poly(azo-ether-imide) nanocomposite films reinforced with nanofibers electrospun from multi-walled carbon nanotube filled poly(azo-ether-imide). *J Plast Film Sheet*. 2013, 30, 266-283
18. de Campos BM, Calefi PS, Ciuffi KJ, de Faria EH, Rocha LA, Nassar EJ, Silva JVL, Oliveira MF, Maia IA. Coating of polyamide 12 by sol-gel methodology. *J Therm Anal Calorim*. 2014, 115, 1029-1035
19. Ali W, Kausar A, and Iqbal T. Reinforcement of High Performance Polystyrene/Polyamide/Polythiophene with Multi-walled Carbon Nanotube Obtained through Various Routes. *Compos Interfaces*. 2015, 22, 885-897
20. Jördens C, Wietzke S, Scheller M, Koch M. Investigation of the water absorption in polyamide and wood plastic composite by terahertz time-domain spectroscopy. *Polym Test*. 2010, 29, 209-215
21. Zhang Q, Li D, Lai D, You Y, Ou B. Preparation, microstructure, mechanical, and thermal properties of in situ polymerized polyimide/organically modified sericite mica composites. *Polym Compos*. DOI: 2015, 10.1002/pc.23402